Journal of Innovative Technology, Vol. 8, No. 1, pp. 1-8, March 2026
http://doi.org/10.29424/JIT.202603_8(1).0001

Environmentally Sustainable Synthesis of Zinc Oxide Nanostructures via Modified Sol-Gel Method for Enhanced Piezoelectric Energy Harvesting Applications

Aman Elahi Khan [1,2], Zahid Ali [3], Zeeshan Aslam Khan [4], Adiqa Kausar Kiani [5*]

ABSTRACT

The high significance of piezoelectric materials has been highlighted recently due to the growing need for sustainable energy harvesting applications. Zinc Oxide among all the particles is of notable interest because it exhibits excellent piezoelectric properties along the [001] crystallographic direction. Perhaps, there lies a dilemma of having synthesizing methods that are both environmentally friendly and affordable with production of high-quality nanostructures with compatible piezoelectric performance. In addressing these challenges, this study fabricated ZnO nanoparticles using a modified sol-gel method while being environmentally sustainable and cost effective. Unlike existing methods that often rely on complex and costly processes or hazardous chemicals, this approach leverages a simplified technique focused on precise substrate preparation to promote the vertical growth of nanorods. We thoroughly characterized the synthesized nanostructures using a suite of analytical techniques. X-ray diffraction (XRD) confirmed a high degree of crystallinity, with a predominant peak corresponding to the c-axis orientation, which is crucial for piezoelectric performance. Scanning electron microscopy (SEM) images revealed the successful formation of vertically aligned nanorods with diameters of approximately 1 μm, a morphology essential for effective charge separation and output. Energy-dispersive spectroscopy (EDS) analysis further validated the high purity of the synthesized material, confirming the absence of unwanted impurities. With this ZnO nanostructure, a piezoelectric nanogenerator (PENG) was fabricated and its performance was evaluated under mechanical stress. The device demonstrated a remarkable peak output voltage of up to 0.75 V, a significant improvement over values typically reported for similar nanostructures. This result demonstrates the practical efficacy of our synthesis method and device design in enhancing the efficiency of energy harvesting. The findings lay a strong foundation for future advancements in piezoelectric devices for applications in wearable electronics, biomedical sensors, and other smart technologies.

Keywords: Zinc oxide nanoparticles; Sol-gel synthesis; Piezoelectric nanogenerator; Energy harvesting; Vertical nanorods; Sustainable nanotechnology

1. INTRODUCTION

The field of nanotechnology continues to yield groundbreaking materials with unique properties, unlocking opportunities for diverse applications in science and engineering. Among these materials, zinc oxide (ZnO) emerges as a particularly promising candidate due to its distinctive piezoelectric characteristics at the nanoscale.

Zinc oxide (ZnO) is made up of zinc metal (Zn) and oxygen (O). It is a solid often found in powdered form and is of white in color. Having a range of physical and chemical characteristics allows this material to be used in various industrial applications [1]. The diameter of this material lies in the typical 100nm range. The catalytic activity of ZnO is high and its Surface Area to Volume ratio can be varied, with different methods of preparation. Its excitation dissociation energy is 60 meV, that is a fairly large value, and the energy of the band gap is relatively wide, with a magnitude of 3.2 eV at r.t.p . To be used in optical and electronic devices, ZnO has the above qualities and more than that, a well-developed epitaxial growth process. It is a suitable material to piezoelectric devices if the substrate has nanowires grown along c-axis, or the (002) direction.

ZnO in crystal form lacks an inversion center, which means it is non-centrosymmetric with polar surfaces and has a wurtzite shape [2]. This structure of zinc oxide is made up by 2 penetrating (hcp) sub lattices of zinc cation and oxygen anion. These are displaced along the c-axis by the length of the bond between the cation and anion. a=3.25 Å and c=5.206 Å are the values of lattice constants of ZnO. As ZnO is comprised of two elements with dissimilar atoms, the lattice constant's c/a of hcp unit has a value of

Manuscript received July 19, 2025; revised September 23, 2025; accepted October 4, 2025.

[1] Graduate Student, Department of Physics and Applied Mathematics, Pakistan Institute of Engineering and Applied Sciences (PIEAS), Islamabad 45650, Pakistan.

[2] Graduate Student, International Graduate School of Artificial Intelligence, National Yunlin University of Science and Technology, Taiwan, R.O.C.

[3] Associate Professor, Materials Division, National Institute of Lasers and Optronics College, Pakistan Institute of Engineering and Applied Sciences (NILOP-C, PIEAS), Nilore, Islamabad, Pakistan

[4] Associate Professor, International Graduate School of Artificial Intelligence, National Yunlin University of Science and Technology, Taiwan, R.O.C.

[5*] Professor (corresponding author), Future Technology Research Center National Yunlin University of Science and Technology, Taiwan, R.O.C. (email: adiqa@yuntech.edu.tw)

8/5; a bit lower than ideal hcp value of 1.633. In the ideal wurtzite structure, a single type of atom is displaced relative to others along the threefold c-axis by a fractional value of u=0.38 within a single hexagonal close-packed (hcp) unit. The displacement value, u, is expressed in fractional coordinates and shows the c-axis's bond length, measured in terms of the lattice parameter c, or alternatively, the nearest-neighbor distance divided by c. Additionally, the bond angles α and β are approximately 109.07º, as illustrated in Figure 1, which pertains to the ideal wurtzite structure.

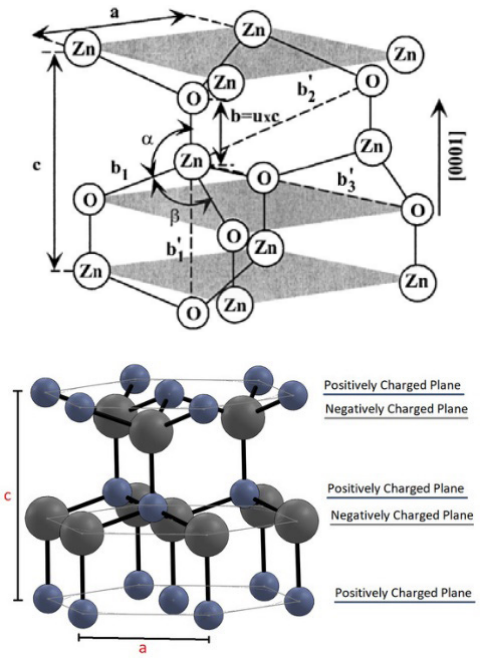

Fig. 1 Wurtzite structure to zinc oxide nanoparticle

There are both extrinsic and intrinsic effects associated with a semiconductor's optical characteristics. Valence band holes and conduction band electrons undergo intrinsic optical transitions, which contain excitation effects brought on by the Coulomb interaction. Equilibrium group velocities between electrons and holes are a prerequisite for exciton formation. There are two main types of excitons: bound excitons and free excitons. Free excitons can exhibit excited states as well as transitions from the ground state, particularly in high-quality samples with minimal impurities. The term 'extrinsic properties' describes the influence of dopants or defects, which generally introduce unique electronic states within the band gap, thereby impacting optical emission and absorption processes.

Stated previously, Zinc Oxide is a transparent conductive material and a direct band semiconductor. The wavelength is of the range of 0 to 3 and 2 to 5 μm. It is where ZnO films are transparent, and depending on the concentration of the carrier, the plasma edge lies in the range of 2 and 4 μm. It is commonly known that when the concentration of carriers increases, the band gap edge shifts. We refer to this shift as the Burstein-Moss shift. Numerous experimental methods are employed to study the variations in the optics of ZnO, including calorimetric spectroscopy, photonic absorption, conduction, reflection, photo-reflection, spectroscopic ellipsometry, photoluminescence, and cathodoluminescence. At room temperature and pressure, the zinc oxide photoluminescence spectrum initially consists of two vital emission bands, the near UV, which lies in 375nm, and the green 150 nm bands [3]. Although a yellow-orange band at 610 nm is occasionally observed, it is low in intensity. Since being tied to the material excitation properties, the near UV emission is particularly important. This includes replicas of photon as well as bound and free exciton emission. Even at low temperatures, luminescence from exciton observation is typically challenging. Numerous factors contribute to this.

Zinc oxide is widely used in optoelectronic and electronic devices due to its properties as a direct band-gap semiconductor with a relatively large band-gap and a binding energy of 60 meV, which is considerable for many applications. Devices made from such materials often have a high breakdown voltage, generate minimal noise, and can operate at high temperatures, even under high-power conditions. The behavior of electron transport in semiconductors changes depending on the strength of the applied electric field. At lower electric field strengths, the energy distribution of electrons in zinc oxide remains nearly unchanged, as the electrons cannot gain much energy from the applied electric field compared to the thermal energy. This results in a constant electron mobility, as the scattering rate remains steady. As the electric field strength increases, the energy of the electrons reaches a point where it matches their thermal energy, causing a significant shift in the electron distribution function. When the temperature exceeds the lattice temperature, the electrons are considered hot electrons, and during this critical period, there is little energy loss to the lattice. Devices with higher frequencies can be designed when the electron's drift velocity exceeds its steady-state value.

Research on the application of zinc oxide in piezoelectric energy harvesters, particularly lead-free piezoelectric materials, is ongoing. These materials can potentially exhibit much stronger piezoelectric properties at the nanoscale than in bulk form. The piezoelectric strain constant, or d33, which measures the ratio of strain to the electric field (m/V) or the charge generated per unit area to the applied stress (C/N), is a key property in piezoelectric materials [4]. While lead zirconate titanate (PZT) ceramics exhibit d33 coefficients in the range of 300 to 600 pm/V, depending on the type of PZT, bulk zinc oxide (BZO) has a d33 of around 12 pm/V. For pure ZnO nanostructures, d33 values range from 0.4 to 80.8 pm/V, with the highest values found in nanosheets (NSs), followed by nanorods (NRs), and then nanobelts. The length (L) and diameter (Φ) of the nanowires (NWs) play a role in determining these values [5].

Due to their unique physical and chemical properties, nanoparticles of ZnO are among the most widely used nanoparticles in drug delivery, cancer diagnosis, and treatment [6]. Apart from being used in the treatment of cancer, ZnO NPs have shown great promise in treating a varied range of other illnesses and in a number of other industries, involving textiles, electronics, and cosmetics. Since ZnO NPs are inexpensive, safe, and easy to prepare, they are the most noteworthy of the inorganic metal oxides that have been produced and are currently being researched. Additionally, any representative intended for human use in the treatment of various disorders must possess the following qualities. ZnO NPs have an above-average biocompatibility, making them suitable for use in a beneficial environment for their antifungal, antibacterial, anticancer, and antiviral qualities. Aside from not being toxic, it should not react with food or the container, taste good or tasteless, and have an unpleasant odor.

Furthermore, ZnO is also suitable for gas sensing applications, such as being used in an alcohol sensor [7]. At 150°C, the ZnO showed the highest response of 15, which was towards H2S. At 100°C, the response was 3, towards NH3, 2 at 50°C, and there was no response to CO2. This indicates that the pure ZnO thick

film sensor is not affected by CO2, NH3, or LPG [8]. Numerous reports describe the sensor's gas-sensing mechanism.

Other than that, ZnO has been reported to show excellent piezoelectric behavior, and its vertically well-aligned nanorods can be effectively used to synthesize piezoelectric nanogenerators [9]. It is reported that when a 4 Newton force at a frequency of one to five Hz is applied on the single-layered PENGs, a voltage of 11V is produced, this output voltage increases on increasing frequency and the improvement in the produced voltage with the applied frequency initiates from the effect of early speed during impact [9].

Zinc oxide nanoparticles exhibit effective piezoelectric properties according to several researchers. While fabrication of piezoelectric materials, there is a broad choice of substrates, but the inexpensive one is the substrate of zinc oxide. Zakariya et al. [10] reports that for surface acoustic wave detection piezoelectric layer is quite crucial. The advantage of using ZnO in this research is that it is a n-type semiconductor and it used for many devices considering its sensitivity and simple doping to enhance sensing capability. In this research, two types of sources were used for deposition: granular and pellet sources. Then the sources were spin-coated onto the substrate, and it was annealed at 500 ℃ for 2 hours. The AFM showed cone-like topography with average roughness of 20.3 nm and 546 nm grain size using pallet source and Ra 28.74 nm and 1029 nm grain size for granular source. For the Sol-Gel analysis the samples exhibit 2θ peak at 31.8°, 34.3° and 36.4°, and 47.6°. Perhaps, at 34.4° the peak with the strongest intensity was perceived that linked to preferred (002) c-axis ZnO crystal alignment. When ZnO reflection peaks are present, the thin film creates the ideal orientation of c-axis for piezoelectric thin films. The average ZnO particle size increased with higher annealing temperatures, as determined by SEM analysis. The range wavelength in the UV-VIS analysis is between 300 and 400 nm, with a band gap of 3.3 eV. According to the results, the best layer in terms of coarseness and absorbance is the granular source. The SAW Biosensor application can take advantage of these ZnO thin films.

Many reports show that zinc oxide NPs prepared by sol gel method have resulted in controlled particle size and improved crystallinity. Hasnidawani [11] prepared ZnO NPs using sodium hydroxide and zinc acetate. Distilled water was utilised as reagent medium and zinc acetate as a precursor. The XRD figure of the prepared ZnO powder showed sharp peaks which imply crystallinity in nature [12]. The two highest peaks were located at an angle of 33.86° at (101) plane with intensity 4847.45 and an angle of 36.27° at an angle of 4069.8. Zinc oxide, comprising 63% of the chemical, was generated as ZnO nanopowder. The results indicated that the Zinc Oxide rod-like structure was successfully made with the use of sol-gel technique, where the size of the particle lay in the nanoscale range, approximately 84.98 nm. The resulting nanoparticles of ZnO demonstrated excellent crystallinity. Alvarado et al. [13] in 2013 synthesized ZnO NPs by the sol-gel method and the spin coating technique with methanol as a reagent and Zinc acetate as a precursor. The thin film of zinc oxide formed by the sol-gel process is a system of layers. Yet, as this work has shown, the ZnO thin film that results from providing the film with an appropriate annealing treatment—that is, the right temperature and duration—has an interface between nearby nanoparticles and has actually formed an entire layer of nanoparticles. Thin films are with preference oriented along the c-axis, as indicated by the nanoparticle morphology. The most thermodynamically advantageous growth direction is along the c-axis orientation, which is named after the (002) plane due to its minimum surface energy. Perfilometry was used to analyze the thickness of the films obtained in this work. It was observed that the maximum thickness of 3600 nm was reached by depositing 30 layers, while the minimum thickness of 200 nm was obtained by depositing a film of 5 layers. Because of the 002 plane's lower energy, the deposited nanoparticles are preferentially oriented near its *c*-axis, resulting in an optical transmittance of up to 75%.

It has been demonstrated that doping ZnO nanoparticles can promote highly oriented vertical growth and improve piezoelectric efficiency. Liu et al. [14] showed that doping and interfacial modifications have a combined positive impact on ZnO-based piezoelectric nanogenerators (PENGs). In this study, chlorine-doped ZnO nanowire (NW) films were found to be favorably oriented perpendicular to the material or substrate. X-ray diffraction (XRD) measurements were employed to analyze the lattice structures of both CI-doped and non-doped ZnO (nanowire) films. All chlorine-doped samples exhibited ZnO (002) peaks that shifted progressively compared to the undoped ZnO sample, which was grown without NaCl in the solution. As the concentration of NaCl in the nutrient solution increased (4, 8, and 10 mM), the ZnO (002) peaks shifted to lower diffraction angles. This shift provided evidence of chlorine incorporation and modification of the lattice parameters in the doped ZnO, in contrast to the undoped ZnO. Based on the diffraction data, the lattice spacings for the undoped ZnO and the Cl-doped ZnO (with 10 mM NaCl) were found to be 5.206 Å and 5.221 Å, respectively.

For reasons of both occupational and road safety, it is critical to identify the brain's alcohol content. As a quick way to gauge the degree of alcohol poisoning impairment, blood alcohol concentration (BAC), which is the proportion of alcohol in the blood, is used to quantify the amount of alcohol in the brain tissues. Xu et al. [7] investigated how ZnO nanoparticles, nanorods, and other materials sensed LPG gas, H_2S, CO, H_2, and Cl_2. ZnO nanorods are more sensitive to LPG than to N2 and CO2, while ZnO nanoparticles are more sensitive to H_2S compared to CO, H_2, etc. The ZnO nanostructure on multilayer graphene upon exposure to 100 ppm of acetone shows a response value of 35.8.

In gas sensing, ZnO nanoparticle interconnectivity is more important than particle size and the surface-to-volume ratio. After the test, gas molecules are adsorbed and desorbed from the sample surface, ZnO nanoparticles can create ionic species there. Important factors to consider when assessing the sensor's potential uses are response and recovery times. The ZnO nanostructured material responds quickly. A zinc oxide-based sensor may detect changes in the environment as a result of test gas molecules' adsorption and desorption (a surface defect). When heated, the ZnO nanoparticle sensor exhibits a significant chemical affinity for certain gas molecules. Oxygen atoms are adsorbed into the ZnO surface prior to exposure to the host gas; they remove electrons from the surface and transform into O− (release oxygen). On the host surface, this O-ion contributes to the formation of the depletion layer. More oxygen may be absorbed as a result, and sensory responses are therefore identified.

The creative inclusions of the study are presented below:

- To explore the nanostructure of ZnO through innovative methods.
- To study its characterizations using XRD, SEM for surface morphology and topology.
- Using acid to evaluate its effects on the structure, electrical properties.
- Performing Raman and EDS to confirm the presence of our substance ZnO.
- Apply the substrate in optimized form on the piezoelectric nanogenerator.

• Analyze piezoelectric and reverse piezoelectric effects.

The residual sections of this research are structured as follows: In 2nd section, the materials and equipment used throughout the project are discussed, along with the method and procedures followed to prepare a Piezoelectric Nanogenerator using Zinc Oxide. Moreover, some of the characterization techniques used to study the material are also briefly discussed. Section 3 deals with the results of the characterization of our material, along with an analysis of those results. The final conceptions are encapsulated in section 4 with an introduction to viable future directions.

2. TECHNIQUE AND MATERIALS

Materials Utilized:

- Zinc nitrate hexahydrate (Zn(NO3)2. 6 H2O, 98%, Riedel de Haen, Germany) (Zinc precursor)
- Methanol with 99.8% purity from Sigma Alrdich, USA.(Solvent)
- Zinc acetate dihydrate (Zn(CH3COO)2 · 2H2O) , Sigma Aldrich, USA. (Zinc precursor)
- Glass Substrate
- Indium tin oxide coated PET substrate with surface resistivity 60Ω/sq by Sigma Aldrich, USA.
- Potassium Hydroxide Pellets by Riedel de Haen, Germany. (Precipitating Agent / pH Modifier)
- De ionized Water (H2O). (solvent)

Equipment:

- Hot plate with magnetic stirrer (Wise Stir MSH 20 A)
- Beam Balance (SHIMADZU ATX-224)
- Vacuum Oven (Gallenhamp)
- Spin Coater VTC 50-A
- Industrial Furnace
- Dropper
- Beaker
- Thermometer
- Aluminum foil and petri dish
- Thin film holder
- CRO
- Multimeter
- Wires
- Conducting Tape
- Plastic sheet

Experimental technique:

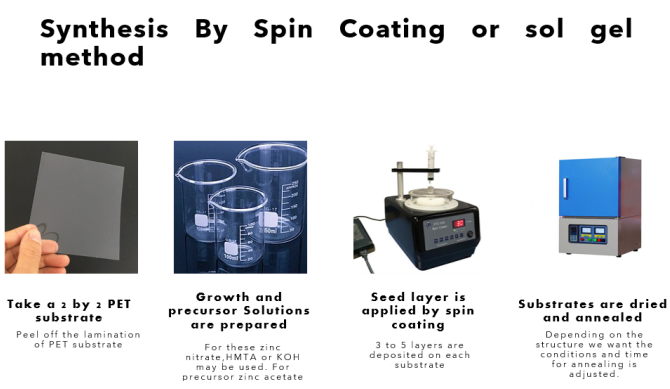

Fig. 2 Steps diagram of experimental technique used.

Zinc Oxide on PET substrate by sol gel method:

ZnO NPs were prepared by the sol-gel method, and for that purpose, 0.021g zinc acetate was mixed in methanol with constant stirring at 60°C for 3 hours and 30 minutes. This was the seed-layer solution. For growth solutions, 0.03M Zinc nitrate was used with 0.03M potassium hydroxide. The exact masses were 0.89g zinc nitrate in 100 mL of DI water and 0.168g potassium hydroxide in 100 mL of DI water. Now, a 2x2 sheet of PET substrate was cut, and its lamination was removed from the conducting side, and a seed layer of zinc acetate in methanol was spin-coated on it using a dropper. The settings of the spin coater were 300rpm for the first 10 seconds and 3000 rpm for the next 60 seconds. With these settings, 3 subsequent seed layers were applied on the substrate with drying at 60°C after each coating. After that, equal volumes of growth solutions were mixed in a beaker, and the PET substrate with the seed-layer was immersed in the growth solutions and was grown at 80°C for 2 hours, and was later dried in the furnace at 80°C for 2 hours. At the end, a small portion of the substrate was cut and was characterized, and the other part was used in making Piezoelectric nanogenerator. In PENG, PET substrate with ZnO nanowires is placed at bottom and another layer of bare PET substrate is placed at the top and the electrical wires are attached to both by conducting tape and the whole device is then covered with medical tape [15] and finally Piezoelectric effect was measured with a multimeter and Cathode Ray Oscilloscope.

Fig.3 Schematic Images from Lab Substrates and IV measurement on left and PENG on Right.

Characterization Techniques

Before the construction of the device, a small piece of substrate was cut and characterized by various characterization techniques, which included Raman Spectroscopy, SEM Analysis, EDS Analysis, XRD, and IV measurements using a Cathode Ray Oscilloscope.

Raman Spectroscopy

Raman Spectroscopy is a non-invasive method for chemical analysis that offers a brief idea of lattice structure, phase, and polymorphisms, molecular relationship, and crystallinity of the material. This technique relies on the mixing of light with the chemical bonds present in the substance [16].

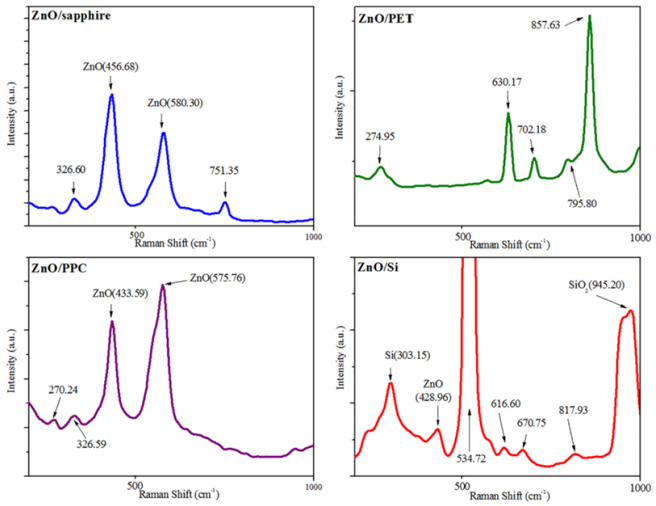

Fig. 4 Some Examples of Raman Shifts of ZnO grown on various substrates [17].

Scanning Electron Microscopy (SEM)

It was performed with FESEM, MAIA-3, and TESEAN. SEM is used for studying the microstructure and morphology of nanomaterials. In this technique, an electron beam with a moderate amount of energy is irradiated onto the material, resulting in a scan in image form after several interactions and the emission of photons and electrons from or near the material's surface [17].

Energy Dispersive Spectroscopy EDS

A scanning electron microscope, combined with an energy-dispersive X-ray system, enables chemical analysis of samples displayed on the screen. The SEM utilizes secondary and back-scattered electrons to create images that reveal the sample's morphology. Additionally, the EDS system identifies and quantifies elements present in the sample by detecting X-rays emitted when the sample is struck by the electron beam, allowing for the analysis of chemical composition at detectable concentrations [18].

X-ray Diffraction (XRD)

XRD is a technique where the sample does not need to be destroyed, tells us about the phases, structures, preferred crystalline orientations, such as texture, and also tells us about the size of the particle synthesized, the defects of the lattice [19]. XRD peaks are produced by the interference (constructive) of a monochromatic beam of X-rays scattered at specific angles from each set of lattice planes in a sample. These peaks are like a fingerprint of a material with standards established such as JCPDS cards for the correct assumption of the material.

3. RESULTS AND DISCUSSION

3.1 Inquiry of XRD

The X-ray diffraction of ZnO on glass substrate shows us sharp peaks, and by using the Sherrer equation, the particle size was found to be an average of 7nm. The comparison from literature and scholarly articles shows us that peak labelled (111) is of bare ITO glass substrate [20] and rest are of the zinc oxide [21].

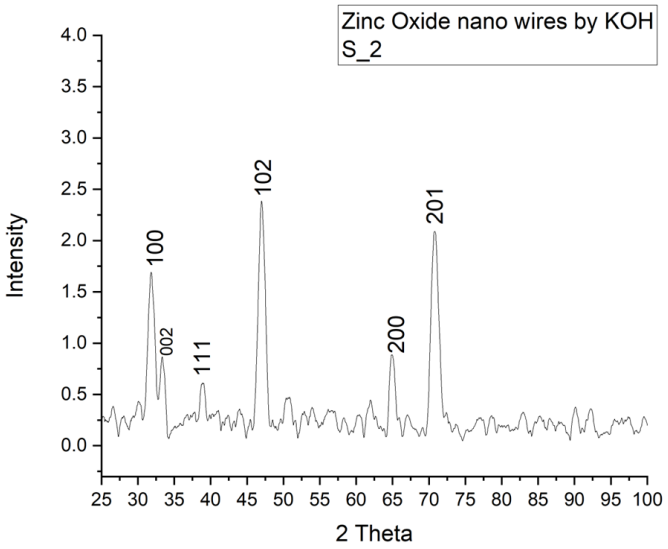

Fig. 5 XRD of ZnO nanorods grown on Glass substrate.

3.2 Analysis of SEM and EDS

The SEM result shows nanorods from above, the first 2 images at top show SEM at 2 and 5µm and the bottom are at larger magnification of about 500nm and in the images we can see the hairs of ZnO nano-rods which are of the size 1 to 2µm and have subsequent spaces between them which means the wires are grown vertically with adequate spaces and the morphology is almost circular or flower like.

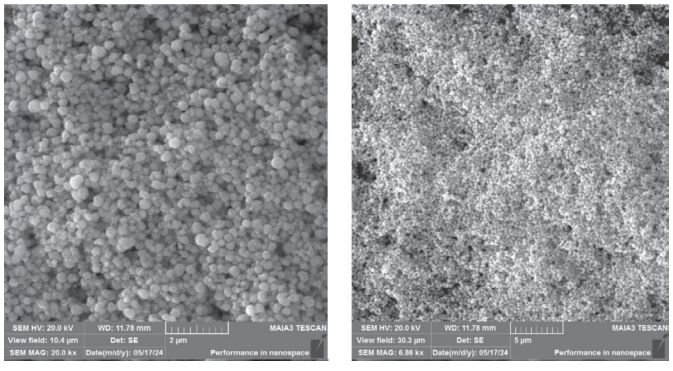

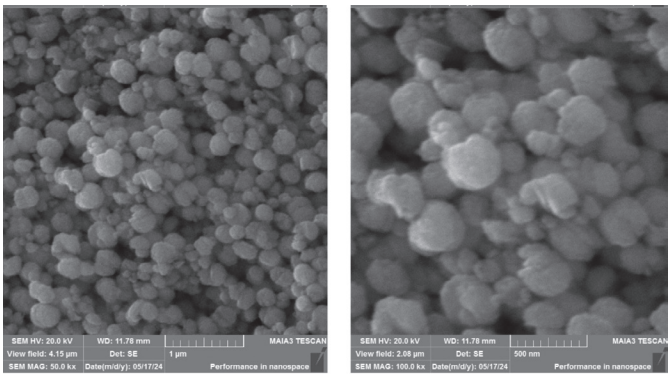

Fig. 6 Top two SEM images at 5 and 2 µm scale and bottom two are at 1µm & 500nm scale.

3.3 Inquiry of EDS

Figure 7 below shows the EDS analysis of ZnO nanorods grown on PET substrate, it is observed that there is no other substance than Zinc, Oxygen and Indium which concludes that there are no unwanted impurities present in our sample.

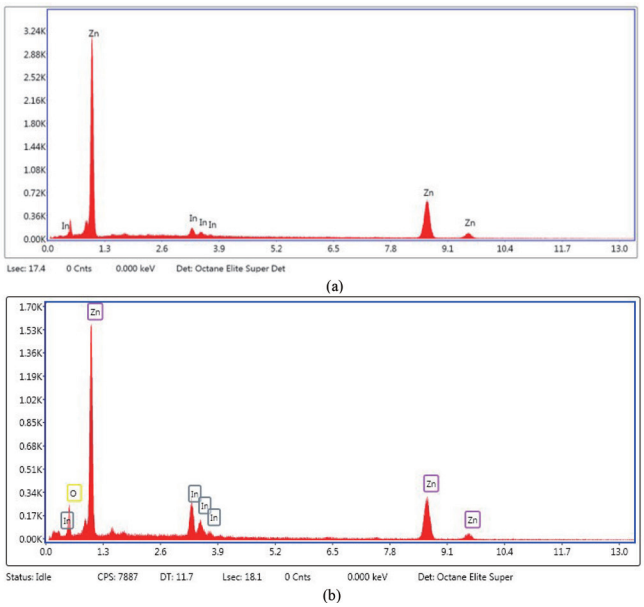

Fig. 7 EDS spectra of ZnO on PET Substrate (Indium Oxide coated)

Element	Weight %	Atomic %	Net Int.	Error %	Kratio	Z	R	A	F
O K	9.48	31.87	94.14	13.43	0.0240	1.2936	0.8360	0.1957	1.0000
InL	17.84	8.36	270.47	7.69	0.1568	0.8766	1.1118	0.9707	1.0326
ZnK	72.67	59.77	536.74	3.86	0.7509	0.9899	1.0013	0.9900	1.0544

(a)

Element	Weight %	Atomic %	Net Int.	Error %	Kratio	Z	R	A	F
InL	4.97	2.89	113.06	16.65	0.0438	0.8910	1.1048	0.9434	1.0482
ZnK	95.03	97.11	1068.24	3.12	0.9979	1.0069	0.9971	0.9967	1.0462

(b)

Fig. 8 Atomic percentage by weight of the composition of the material

The EDS tables of the samples show that only Zinc and Oxygen are present in the material and there is 4.97 atomic percentage by weight indium in sample at spot 1 and 17.84 percent at spot 2 this impurity is the result of coating of Indium on our PET substrate and no unwanted impurity is recorded.

3.4 Raman Analysis

The attachment below is the Raman shift plot of ZnO nanorods synthesized and grown on the PET substrate the data when compared with literature, shows [22] us that the peaks at 623 and 853 correspond to the Raman Shifts of ZnO and the rest of the peaks 1276, 1600 and 1712 are of the bare PET substrate [23]. However, there is an overlap of Raman shifts of PET and ZnO, but the results here show the peaks matching our materials.

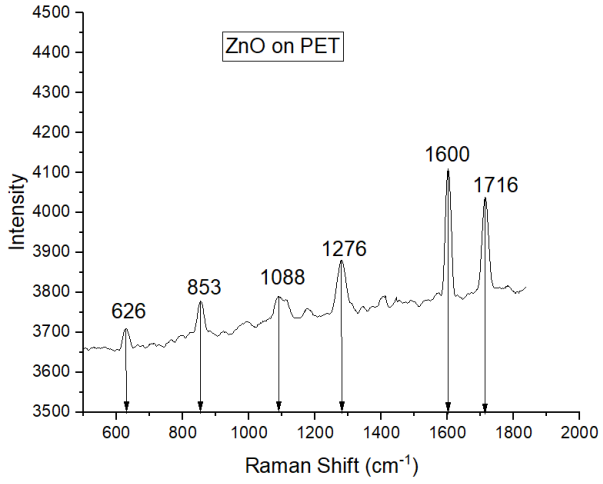

Fig. 9 Raman Shift plots of ZnO nanorods on PET (Indium coated) Substrate.

3.5 Voltage Measuement

First for control experiment the CRO was run with sinusoidal AC voltage without applied force the PENG then Voltage was measured with attaching the device with cathode ray oscilloscope and the piezoelectric part was provided the constant force [24] and upto 0.75v was measured, hence confirming the piezoelectric effect. The readings were taken after one and then two days of material synthesis so that sustainability is assured [25].

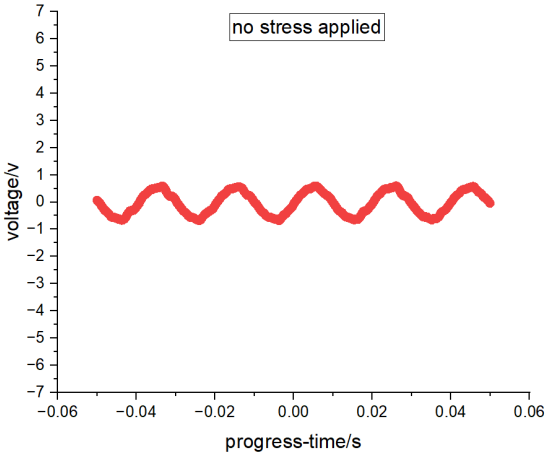

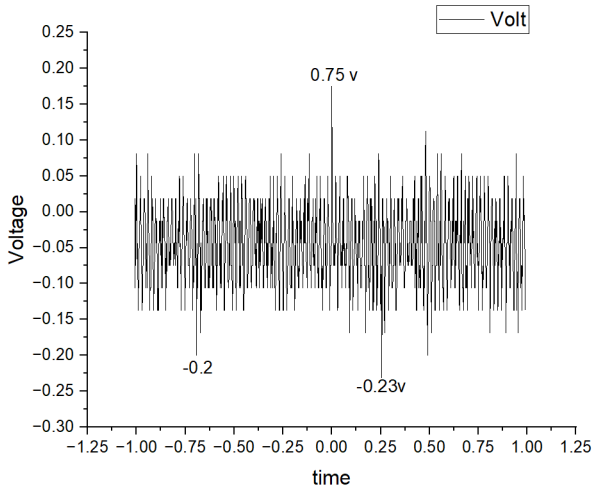

Fig. 10 Top: Voltage amplitude spike at 50hz frequency. Bottom: voltage peaks measurement when the force is applied.

4. CONCLUSION AND FUTURE WORK

In this study, ZnO was successfully synthesized by different growth solutions such as HMTA, Zinc nitrate, and KOH on different substrates such as ITO glass, then FTO glass, and finally on a plastic substrate. The XRD characterizations of the samples showed that high-temperature annealing increases crystallinity but also increases particle size. The morphology of ZnO on PET is of platelets, with almost no overlapping, showing a zinc acetate seed layer, and potassium hydroxide and zinc nitrate are optimal for wire growth. The EDS confirmed the purity of our sample. Furthermore, the goal was to demonstrate the piezoelectric effect of the material in device form, which was achieved. The readings suggest that one time tapping the substrate yields a voltage of up to 0.5 to 1 volt. The PNG produces a dc current in one direction in compression mode and in the opposite direction in relaxation mode in response to mechanical force, whereas the maximum voltage reaches 0.7V [26]. The voltage varies depending on what specific mode is being measured and the amount of force that's applied. Next, we plan to study more on these materials, make them more sensitive, and at the root of making the growth of nanowires as vertical as possible, and their morphology to be as thin as possible, so that a slight vibration can generate enough current to run a device. The uses of these piezoelectric substances are enormous, such as pacemakers for the heart, ultra-sensitive microphones, smart door locks, and a piezoelectric Bluetooth keyboard. We have an ambition to manufacture these devices for both vehicles and domestic homes. The relevant field of work on green nanomaterials can be further collaborated with artificial intelligence using different machine learning techniques to optimize the vertical growth of zinc oxide nanowires and identify the best wurtzite structure for maximum voltage output in future work. In this aspect, the fractional model applied to machine learning techniques can prove insightful in biomedical sensors and nanodevices, i.e, (piezoelectric pacemaker) as demonstrated in the following references [27-34].

References

[1] R. K. Pandey, J. Dutta, S. Brahma, B. Rao, and C. P. Liu, "Review on ZnO-based piezotronics and piezoelectric nanogenerators: Aspects of piezo potential and screening effect," *JPhys Materials,* vol. **4**, no. 4, Oct. 2021, doi: 10.1088/2515-7639/ac130a.

[2] Ü. Özgür et al., "A comprehensive review of ZnO materials and devices," *Journal of Applied Physics,* vol. **98**, no. 4. pp. 1–103, Aug. 15, 2005. doi: 10.1063/1.1992666.

[3] L. Stolt, J. Hedström, J. Kessler, M. Ruckh, K. O. Velthaus, and H. W. Schock, "ZnO/CdS/CuInSe2 thin-film solar cells with improved performance," *Appl Phys Lett,* vol. **62**, no. 6, pp. 597–599, 1993, doi: 10.1063/1.108867.

[4] N. Bhadwal, R. Ben Mrad, and K. Behdinan, "Review of Zinc Oxide Piezoelectric Nanogenerators: Piezoelectric Properties, Composite Structures and Power Output," *Sensors,* vol. **23**, no. 8. MDPI, Apr. 01, 2023. doi: 10.3390/s23083859.

[5] W. Troy, M. Dutta, and M. Stroscio, "Spontaneous polarization calculations in wurtzite ii-oxides, iii-nitrides, and sic polytypes through net dipole moments and the effects of nanoscale layering," *Nanomaterials,* vol. **11**, no. 8, Aug. 2021, doi: 10.3390/nano11081956.

[6] S. Anjum et al., "Recent advances in zinc oxide nanoparticles (Zno nps) for cancer diagnosis, target drug delivery, and treatment," *Cancers (Basel),* vol. **13**, no. 18, Sep. 2021, doi: 10.3390/cancers13184570.

[7] Xu J, Han J, Zhang Y, Sun YA, Xie B. Studies on alcohol sensing mechanism of ZnO based gas sensors. Sensors and Actuators B: Chemical. 2008 May 28;132(1):334-9.

[8] S. G. Onkar, S. B. Nagdeote, A. S. Wadatkar, and P. B. Kharat, "Gas sensing behavior of ZnO thick film sensor towards H2S, NH3, LPG and CO2," in Journal of Physics: Conference Series, IOP Publishing Ltd, Oct. 2020. doi: 10.1088/1742-6596/1644/1/012060.

[9] P. Fakhri, N. Eaianli, R. Bagherzadeh, B. Jaleh, M. Kashfi, and R. Fausto, "Sandwich-type double-layer piezoelectric nanogenerators based on one- and two-dimensional ZnO nanostructures with improved output performance," *Sci Rep,* vol. **13**, no. 1, Dec. 2023, doi: 10.1038/s41598-023-43047-4.

[10] M. R. Zakaria, S. Johari, M. H. Ismail, and U. Hashim, "Characterization of Zinc Oxide (ZnO) piezoelectric properties for Surface Acoustic Wave (SAW) device," *in EPJ Web of Conferences, EDP Sciences,* Nov. 2017. doi: 10.1051/epjconf/201716201055.

[11] J. N. Hasnidawani, H. N. Azlina, H. Norita, N. N. Bonnia, S. Ratim, and E. S. Ali, "Synthesis of ZnO Nanostructures Using Sol-Gel Method," *Procedia Chem,* vol. **19**, pp. 211–216, 2016, doi: 10.1016/j.proche.2016.03.095.

[12] S. Rezabeigy, M. Behboudnia, and N. Nobari, "Growth of ZnO Nanorods on Glass Substrate by Chemical Bath Deposition," *Procedia Materials Science,* vol. **11**, pp. 364–369, 2015, doi: 10.1016/j.mspro.2015.11.130.

[13] J. A. Alvarado, A. Maldonado, H. Juarez, and M. Pacio, "Synthesis of colloidal ZnO nanoparticles and deposit of thin films by spin coating technique," *J Nanomater,* vol. **2013**, 2013, doi: 10.1155/2013/903191.

[14] C. Liu et al., "Improvement in the Piezoelectric Performance of a ZnO Nanogenerator by a Combination of Chemical Doping and Interfacial Modification," *Journal of Physical Chemistry C,* vol. **120**, no. 13, pp. 6971–6977, Apr. 2016, doi: 10.1021/acs.jpcc.6b00069.

[15] S. Das Mahapatra et al., "Piezoelectric Materials for Energy Harvesting and Sensing Applications: Roadmap for Future Smart Materials," *Advanced Science,* vol. **8**, no. 17. John Wiley and Sons Inc, Sep. 01, 2021. doi: 10.1002/advs.202100864.

[16] S. H. Ribut, C. A. Che Abdullah, and M. Z. Mohammad Yusoff, "Investigations of structural and optical properties of zinc oxide thin films growth on various substrates," *Results Phys,* vol. **13**, Jun. 2019, doi: 10.1016/j.rinp.2019.02.082.

[17] M. Omidi et al., "Characterization of biomaterials," *Biomaterials for Oral and Dental Tissue Engineering,* pp. 97–115, Jan. 2017, doi: 10.1016/B978-0-08-100961-1.00007-4.

[18] S. Nasrazadani and S. Hassani, "Chapter 2. Modern analytical techniques in failure analysis of aerospace, chemical, and oil and gas industries," 2016. doi: 10.1016/B978-0-08-100117-2.00010-8.

[19] A. A. Bunaciu, E. gabriela Udriştioiu, and H. Y. Aboul-Enein, "X-Ray Diffraction: Instrumentation and Applications," *Critical Reviews in Analytical Chemistry,* vol. **45**, no. 4. Taylor and Francis Ltd., pp. 289–299, Oct. 02, 2015. doi: 10.1080/10408347.2014.949616.

[20] R. Shan, J. Yi, J. Zhong, and S. Yang, "Effect of sulphur pressure on properties of ZnS thin film prepared by chemical bath deposition technique," *Journal of Materials Science: Materials in Electronics,* vol. **30**, no. 14, pp. 13230–13237, Jul. 2019, doi: 10.1007/s10854-019-01686-2.

[21] H. Mandal et al., "Improved photoelectrochemical water oxidation using wurtzite ZnO semiconductors synthesized through simple chemical bath reaction," *Electrochim Acta,* vol. **14**1, pp. 294–301, Sep. 2014, doi: 10.1016/j.electacta.2014.06.013.

[22] L. Cao, J. Kiely, M. Piano, and R. Luxton, "Facile and inexpensive fabrication of zinc oxide based bio-surfaces for C-reactive protein detection," *Sci Rep,* vol. **8**, no. 1, Dec. 2018, doi: 10.1038/s41598-018-30793-z.

[23] X. Wang et al., "Flexible graphene field effect transistor with ferroelectric polymer gate," *Opt Quantum Electron,* vol. **48**, Jun. 2016, doi: 10.1007/s11082-016-0614-y.

[24] M. S. Al-Ruqeishi, T. Mohiuddin, B. Al-Habsi, F. Al-Ruqeishi, A. Al-Fahdi, and A. Al-Khusaibi, "Piezoelectric nanogenerator based on ZnO nanorods," *Arabian Journal of Chemistry,* vol. **12**, no. 8, pp. 5173–5179, Dec. 2019, doi: 10.1016/j.arabjc.2016.12.010.

[25] J. Briscoe et al., "Measurement techniques for piezoelectric nanogenerators," *Energy Environ Sci,* vol. **6**, no. 10, pp. 3035–3045, Oct. 2013, doi: 10.1039/c3ee41889h.

[26] H. Mandal et al., "Improved photoelectrochemical water oxidation using wurtzite ZnO semiconductors synthesized through simple chemical bath reaction," *Electrochim Acta,* vol. **141**, pp. 294–301, Sep. 2014, doi: 10.1016/j.electacta.2014.06.013.

[27] Ali, M.A., Chaudhary, N.I., Khan, T.A., Mao, W.L., Lin, C.C. and Raja, M.A.Z., 2024. "Design of key term separated identification model for fractional input nonlinear output error systems: Auxiliary model based Runge Kutta optimization algorithm." *Chaos, Solitons & Fractals,* **189**, p.115696.

[28] Ali, M.A., Chaudhary, N.I., Khan, T.A., Mao, W.L., Lin, C.C., Khan, Z.A. and Zahoor Raja, M.A., 2025. "Auxiliary Model-Based Chameleon Swarm Optimization for Robust Parameter Estimation of Fractional Order Nonlinear Hammerstein Systems." *Journal of Computational and Nonlinear Dynamics,* **20**(9), p.091005.

[29] Ali, M.A., Chaudhary, N.I., Lin, C.C. and Mao, W.L., 2025. "Mountain Gazelle optimization algorithm for identification of nonlinear Hammer-stein output error systems." *Journal of Innovative Technology,* **7**(1), pp.117-124.

[30] Anwar, N., Ahmad, I., Javaid, H., Kiani, A.K., Shoaib, M. and Raja, M.A.Z., 2025. "Numerical treatment of stochastic Runge-Kutta Solver Brownian probabilistic hepatitis B virus infection model." *Biomedical Signal Processing and Control,* **110**, p.108177.

[31] Anwar, N., Naz, S., Raja, M.A.Z., Ahmad, I., Shoaib, M. and Kiani, A.K., 2025. "Machine learning solutions with supervised adaptive neural networks for countermeasure competing strategy of computer virus models." *Simulation Modelling Practice and Theory,* p.103141.

[32] Anwar, N., Fatima, A., Raja, M.A.Z., Ahmad, I., Shoaib, M. and Kiani, A.K., 2025. "Stochastic Milstein computing driven autoregressive exogenous neuro-architecture for chaotic nonlinear measles transmission system with impact of immunization." *The European Physical Journal Plus,* **140**(4), p.318.

[33] Anwar, N., Saddiq, A., Raja, M.A.Z., Ahmad, I., Shoaib, M. and Kiani, A.K., 2025. "Novel machine intelligent expedition with adaptive autoregressive exogenous neural structure for nonlinear multi-delay differential systems in computer virus propagation." *Engineering Applications of Artificial Intelligence,* **146**, p.110234.

[34] Anwar, N., Ahmad, I., Javaid, H., Kiani, A.K., Shoaib, M. and Raja, M.A.Z., 2025. "Dynamical analysis of hepatitis B virus through the stochastic and the deterministic model." *Computer Methods in Biomechanics and Biomedical Engineering,* pp.1-17.